

Search for Exotic $S = -2$ Baryons in $p\bar{p}$ Collisions at $\sqrt{s} = 1.96$ TeV

A. Abulencia,²⁴ J. Adelman,¹³ T. Affolder,¹⁰ T. Akimoto,⁵⁶ M.G. Albrow,¹⁷ D. Ambrose,¹⁷ S. Amerio,⁴⁴ D. Amidei,³⁵ A. Anastassov,⁵³ K. Anikeev,¹⁷ A. Annovi,¹⁹ J. Antos,¹⁴ M. Aoki,⁵⁶ G. Apollinari,¹⁷ J.-F. Arguin,³⁴ T. Arisawa,⁵⁸ A. Artikov,¹⁵ W. Ashmanskas,¹⁷ A. Attal,⁸ F. Azfar,⁴³ P. Azzi-Bacchetta,⁴⁴ P. Azzurri,⁴⁷ N. Bacchetta,⁴⁴ W. Badgett,¹⁷ A. Barbaro-Galtieri,²⁹ V.E. Barnes,⁴⁹ B.A. Barnett,²⁵ S. Baroiant,⁷ V. Bartsch,³¹ G. Bauer,³³ F. Bedeschi,⁴⁷ S. Behari,²⁵ S. Belforte,⁵⁵ G. Bellettini,⁴⁷ J. Bellinger,⁶⁰ A. Belloni,³³ D. Benjamin,¹⁶ A. Beretvas,¹⁷ J. Beringer,²⁹ T. Berry,³⁰ A. Bhatti,⁵¹ M. Binkley,¹⁷ D. Bisello,⁴⁴ R.E. Blair,² C. Blocker,⁶ B. Blumenfeld,²⁵ A. Bocci,¹⁶ A. Bodek,⁵⁰ V. Boisvert,⁵⁰ G. Bolla,⁴⁹ A. Bolshov,³³ D. Bortoletto,⁴⁹ J. Boudreau,⁴⁸ A. Boveia,¹⁰ B. Brau,¹⁰ L. Brigliadori,⁵ C. Bromberg,³⁶ E. Brubaker,¹³ J. Budagov,¹⁵ H.S. Budd,⁵⁰ S. Budd,²⁴ S. Budroni,⁴⁷ K. Burkett,¹⁷ G. Busetto,⁴⁴ P. Bussey,²¹ K. L. Byrum,² S. Cabrera^o,¹⁶ M. Campanelli,²⁰ M. Campbell,³⁵ F. Canelli,¹⁷ A. Canepa,⁴⁹ S. Carilloⁱ,¹⁸ D. Carlsmith,⁶⁰ R. Carosi,⁴⁷ S. Carron,³⁴ M. Casarsa,⁵⁵ A. Castro,⁵ P. Catastini,⁴⁷ D. Cauz,⁵⁵ M. Cavalli-Sforza,³ A. Cerri,²⁹ L. Cerrito^m,⁴³ S.H. Chang,²⁸ Y.C. Chen,¹ M. Chertok,⁷ G. Chiarelli,⁴⁷ G. Chlachidze,¹⁵ F. Chlebana,¹⁷ I. Cho,²⁸ K. Cho,²⁸ D. Chokheli,¹⁵ J.P. Chou,²² G. Choudalakis,³³ S.H. Chuang,⁶⁰ K. Chung,¹² W.H. Chung,⁶⁰ Y.S. Chung,⁵⁰ M. Ciljak,⁴⁷ C.I. Ciobanu,²⁴ M.A. Ciocci,⁴⁷ A. Clark,²⁰ D. Clark,⁶ M. Coca,¹⁶ G. Compostella,⁴⁴ M.E. Convery,⁵¹ J. Conway,⁷ B. Cooper,³⁶ K. Copic,³⁵ M. Cordelli,¹⁹ G. Cortiana,⁴⁴ F. Crescioli,⁴⁷ C. Cuenca Almenar^o,⁷ J. Cuevas^l,¹¹ R. Culbertson,¹⁷ J.C. Cully,³⁵ D. Cyr,⁶⁰ S. DaRonco,⁴⁴ M. Datta,¹⁷ S. D'Auria,²¹ T. Davies,²¹ M. D'Onofrio,³ D. Dagenhart,⁶ P. de Barbaro,⁵⁰ S. De Cecco,⁵² A. Deisher,²⁹ G. De Lentdecker,^c,⁵⁰ M. Dell'Orso,⁴⁷ F. Delli Paoli,⁴⁴ L. Demortier,⁵¹ J. Deng,¹⁶ M. Deninno,⁵ D. De Pedis,⁵² P.F. Derwent,¹⁷ G.P. Di Giovanni,⁴⁵ C. Dionisi,⁵² B. Di Ruzza,⁵⁵ J.R. Dittmann,⁴ P. DiTuro,⁵³ C. Dörr,²⁶ S. Donati,⁴⁷ M. Donega,²⁰ P. Dong,⁸ J. Donini,⁴⁴ T. Dorigo,⁴⁴ S. Dube,⁵³ J. Efron,⁴⁰ R. Erbacher,⁷ D. Errede,²⁴ S. Errede,²⁴ R. Eusebi,¹⁷ H.C. Fang,²⁹ S. Farrington,³⁰ I. Fedorko,⁴⁷ W.T. Fedorko,¹³ R.G. Feild,⁶¹ M. Feindt,²⁶ J.P. Fernandez,³² R. Field,¹⁸ G. Flanagan,⁴⁹ A. Foland,²² S. Forrester,⁷ G.W. Foster,¹⁷ M. Franklin,²² J.C. Freeman,²⁹ I. Furic,¹³ M. Gallinaro,⁵¹ J. Galyardt,¹² J.E. Garcia,⁴⁷ F. Garberson,¹⁰ A.F. Garfinkel,⁴⁹ C. Gay,⁶¹ H. Gerberich,²⁴ E. Gerchtein,¹² D. Gerdes,³⁵ S. Giagu,⁵² P. Giannetti,⁴⁷ A. Gibson,²⁹ K. Gibson,⁴⁸ J.L. Gimmell,⁵⁰ C. Ginsburg,¹⁷ N. Giokaris^a,¹⁵ M. Giordani,⁵⁵ P. Giromini,¹⁹ M. Giunta,⁴⁷ G. Giurgiu,¹² V. Glagolev,¹⁵ D. Glenzinski,¹⁷ M. Gold,³⁸ N. Goldschmidt,¹⁸ J. Goldstein^b,⁴³ A. Golosyanov,¹⁷ G. Gomez,¹¹ G. Gomez-Ceballos,¹¹ M. Goncharov,⁵⁴ O. González,³² I. Gorelov,³⁸ A.T. Goshaw,¹⁶ K. Goulianos,⁵¹ A. Greselle,⁴⁴ M. Griffiths,³⁰ S. Grinstein,²² C. Grossi-Pilcher,¹³ R.C. Group,¹⁸ U. Grundler,²⁴ J. Guimaraes da Costa,²² Z. Gunay-Unalan,³⁶ C. Haber,²⁹ K. Hahn,³³ S.R. Hahn,¹⁷ E. Halkiadakis,⁵³ A. Hamilton,³⁴ B.-Y. Han,⁵⁰ J.Y. Han,⁵⁰ R. Handler,⁶⁰ F. Happacher,¹⁹ K. Hara,⁵⁶ M. Hare,⁵⁷ S. Harper,⁴³ R.F. Harr,⁵⁹ R.M. Harris,¹⁷ M. Hartz,⁴⁸ K. Hatakeyama,⁵¹ J. Hauser,⁸ A. Heijboer,⁴⁶ B. Heinemann,³⁰ J. Heinrich,⁴⁶ C. Henderson,³³ M. Herndon,⁶⁰ J. Heuser,²⁶ D. Hidas,¹⁶ C.S. Hill^b,¹⁰ D. Hirschbuehl,²⁶ A. Hocker,¹⁷ A. Holloway,²² S. Hou,¹ M. Houlden,³⁰ S.-C. Hsu,⁹ B.T. Huffman,⁴³ R.E. Hughes,⁴⁰ U. Husemann,⁶¹ J. Huston,³⁶ J. Incandela,¹⁰ G. Introzzi,⁴⁷ M. Iori,⁵² Y. Ishizawa,⁵⁶ A. Ivanov,⁷ B. Iyutin,³³ E. James,¹⁷ D. Jang,⁵³ B. Jayatilaka,³⁵ D. Jeans,⁵² H. Jensen,¹⁷ E.J. Jeon,²⁸ S. Jindariani,¹⁸ M. Jones,⁴⁹ K.K. Joo,²⁸ S.Y. Jun,¹² J.E. Jung,²⁸ T.R. Junk,²⁴ T. Kamon,⁵⁴ P.E. Karchin,⁵⁹ Y. Kato,⁴² Y. Kemp,²⁶ R. Kephart,¹⁷ U. Kerzel,²⁶ V. Khotilovich,⁵⁴ B. Kilminster,⁴⁰ D.H. Kim,²⁸ H.S. Kim,²⁸ J.E. Kim,²⁸ M.J. Kim,¹² S.B. Kim,²⁸ S.H. Kim,⁵⁶ Y.K. Kim,¹³ N. Kimura,⁵⁶ L. Kirsch,⁶ S. Klimenko,¹⁸ M. Klute,³³ B. Knuteson,³³ B.R. Ko,¹⁶ K. Kondo,⁵⁸ D.J. Kong,²⁸ J. Konigsberg,¹⁸ A. Korytov,¹⁸ A.V. Kotwal,¹⁶ A. Kovalev,⁴⁶ A.C. Kraan,⁴⁶ J. Kraus,²⁴ I. Kravchenko,³³ M. Kreps,²⁶ J. Kroll,⁴⁶ N. Krumnack,⁴ M. Kruse,¹⁶ V. Krutelyov,¹⁰ T. Kubo,⁵⁶ S. E. Kuhlmann,² T. Kuhr,²⁶ Y. Kusakabe,⁵⁸ S. Kwang,¹³ A.T. Laasanen,⁴⁹ S. Lai,³⁴ S. Lami,⁴⁷ S. Lammel,¹⁷ M. Lancaster,³¹ R.L. Lander,⁷ K. Lannon,⁴⁰ A. Lath,⁵³ G. Latino,⁴⁷ I. Lazzizzera,⁴⁴ T. LeCompte,² J. Lee,⁵⁰ J. Lee,²⁸ Y.J. Lee,²⁸ S.W. Leeⁿ,⁵⁴ R. Lefevre,³ N. Leonardo,³³ S. Leone,⁴⁷ S. Levy,¹³ J.D. Lewis,¹⁷ C. Lin,⁶¹ C.S. Lin,¹⁷ M. Lindgren,¹⁷ E. Lipeles,⁹ A. Lister,⁷ D.O. Litvintsev,¹⁷ T. Liu,¹⁷ N.S. Lockyer,⁴⁶ A. Loginov,⁶¹ M. Loretta,⁴⁴ P. Loverre,⁵² R.-S. Lu,¹ D. Lucchesi,⁴⁴ P. Lujan,²⁹ P. Lukens,¹⁷ G. Lungu,¹⁸ L. Lyons,⁴³ J. Lys,²⁹ R. Lysak,¹⁴ E. Lytken,⁴⁹ P. Mack,²⁶ D. MacQueen,³⁴ R. Madrak,¹⁷ K. Maeshima,¹⁷ K. Makhoul,³³ T. Maki,²³ P. Maksimovic,²⁵

S. Malde,⁴³ G. Manca,³⁰ F. Margaroli,⁵ R. Marginean,¹⁷ C. Marino,²⁶ C.P. Marino,²⁴ A. Martin,⁶¹
 M. Martin,²¹ V. Martin^g,²¹ M. Martínez,³ T. Maruyama,⁵⁶ P. Mastrandrea,⁵² T. Masubuchi,⁵⁶
 H. Matsunaga,⁵⁶ M.E. Mattson,⁵⁹ R. Mazini,³⁴ P. Mazzanti,⁵ K.S. McFarland,⁵⁰ P. McIntyre,⁵⁴
 R. McNulty^f,³⁰ A. Mehta,³⁰ P. Mehtala,²³ S. Menzemer^h,¹¹ A. Menzione,⁴⁷ P. Merkel,⁴⁹ C. Mesropian,⁵¹
 A. Messina,³⁶ T. Miao,¹⁷ N. Miladinovic,⁶ J. Miles,³³ R. Miller,³⁶ C. Mills,¹⁰ M. Milnik,²⁶ A. Mitra,¹
 G. Mitselmakher,¹⁸ A. Miyamoto,²⁷ S. Moed,²⁰ N. Moggi,⁵ B. Mohr,⁸ R. Moore,¹⁷ M. Morello,⁴⁷
 P. Movilla Fernandez,²⁹ J. Mülmenstädt,²⁹ A. Mukherjee,¹⁷ Th. Muller,²⁶ R. Mumford,²⁵ P. Murat,¹⁷
 J. Nachtman,¹⁷ A. Nagano,⁵⁶ J. Naganoma,⁵⁸ I. Nakano,⁴¹ A. Napier,⁵⁷ V. Necula,¹⁸ C. Neu,⁴⁶
 M.S. Neubauer,⁹ J. Nielsen,²⁹ T. Nigmanov,⁴⁸ L. Nodulman,² O. Norniella,³ E. Nurse,³¹ S.H. Oh,¹⁶
 Y.D. Oh,²⁸ I. Oksuzian,¹⁸ T. Okusawa,⁴² R. Oldeman,³⁰ R. Orava,²³ K. Osterberg,²³ C. Pagliarone,⁴⁷
 E. Palencia,¹¹ V. Papadimitriou,¹⁷ A.A. Paramonov,¹³ B. Parks,⁴⁰ S. Pashapour,³⁴ J. Patrick,¹⁷
 G. Paulett,⁵⁵ M. Paulini,¹² C. Paus,³³ D.E. Pellett,⁷ A. Penzo,⁵⁵ T.J. Phillips,¹⁶ G. Piacentino,⁴⁷
 J. Piedra,⁴⁵ L. Pinera,¹⁸ K. Pitts,²⁴ C. Plager,⁸ L. Pondrom,⁶⁰ X. Portell,³ O. Poukhov,¹⁵ N. Pounder,⁴³
 F. Prakoshyn,¹⁵ A. Pronko,¹⁷ J. Proudfoot,² F. Ptohos^e,¹⁹ G. Punzi,⁴⁷ J. Pursley,²⁵ J. Rademacker^b,⁴³
 A. Rahaman,⁴⁸ N. Ranjan,⁴⁹ S. Rappoccio,²² B. Reisert,¹⁷ V. Rekovic,³⁸ P. Renton,⁴³ M. Rescigno,⁵²
 S. Richter,²⁶ F. Rimondi,⁵ L. Ristori,⁴⁷ A. Robson,²¹ T. Rodrigo,¹¹ E. Rogers,²⁴ S. Rolli,⁵⁷ R. Roser,¹⁷
 M. Rossi,⁵⁵ R. Rossin,¹⁸ A. Ruiz,¹¹ J. Russ,¹² V. Rusu,¹³ H. Saarikko,²³ S. Sabik,³⁴ A. Safonov,⁵⁴
 W.K. Sakumoto,⁵⁰ G. Salamanna,⁵² O. Saltó,³ D. Saltzberg,⁸ C. Sánchez,³ L. Santi,⁵⁵ S. Sarkar,⁵²
 L. Sartori,⁴⁷ K. Sato,¹⁷ P. Savard,³⁴ A. Savoy-Navarro,⁴⁵ T. Scheidle,²⁶ P. Schlabach,¹⁷ E.E. Schmidt,¹⁷
 M.P. Schmidt,⁶¹ M. Schmitt,³⁹ T. Schwarz,⁷ L. Scodellaro,¹¹ A.L. Scott,¹⁰ A. Scribano,⁴⁷ F. Scuri,⁴⁷
 A. Sedov,⁴⁹ S. Seidel,³⁸ Y. Seiya,⁴² A. Semenov,¹⁵ L. Sexton-Kennedy,¹⁷ A. Sfyrla,²⁰ M.D. Shapiro,²⁹
 T. Shears,³⁰ P.F. Shepard,⁴⁸ D. Sherman,²² M. Shimojima^k,⁵⁶ M. Shochet,¹³ Y. Shon,⁶⁰ I. Shreyber,³⁷
 A. Sidoti,⁴⁷ P. Sinervo,³⁴ A. Sisakyan,¹⁵ J. Sjolin,⁴³ A.J. Slaughter,¹⁷ J. Slaunwhite,⁴⁰ K. Sliwa,⁵⁷
 J.R. Smith,⁷ F.D. Snider,¹⁷ R. Snihur,³⁴ M. Soderberg,³⁵ A. Soha,⁷ S. Somalwar,⁵³ V. Sorin,³⁶
 J. Spalding,¹⁷ F. Spinella,⁴⁷ T. Spreitzer,³⁴ P. Squillacioti,⁴⁷ M. Stanitzki,⁶¹ A. Staveris-Polykalas,⁴⁷
 R. St. Denis,²¹ B. Stelzer,⁸ O. Stelzer-Chilton,⁴³ D. Stentz,³⁹ J. Strologas,³⁸ D. Stuart,¹⁰ J.S. Suh,²⁸
 A. Sukhanov,¹⁸ H. Sun,⁵⁷ T. Suzuki,⁵⁶ A. Taffard,²⁴ R. Takashima,⁴¹ Y. Takeuchi,⁵⁶ K. Takikawa,⁵⁶
 M. Tanaka,² R. Tanaka,⁴¹ M. Tecchio,³⁵ P.K. Teng,¹ K. Terashi,⁵¹ J. Thom^d,¹⁷ A.S. Thompson,²¹
 E. Thomson,⁴⁶ P. Tipton,⁶¹ V. Tiwari,¹² S. Tkaczyk,¹⁷ D. Toback,⁵⁴ S. Tokar,¹⁴ K. Tollefson,³⁶
 T. Tomura,⁵⁶ D. Tonelli,⁴⁷ S. Torre,¹⁹ D. Torretta,¹⁷ S. Tourneur,⁴⁵ W. Trischuk,³⁴ R. Tsuchiya,⁵⁸
 S. Tsuno,⁴¹ N. Turini,⁴⁷ F. Ukegawa,⁵⁶ T. Unverhau,²¹ S. Uozumi,⁵⁶ D. Usynin,⁴⁶ S. Vallecorsa,²⁰
 N. van Remortel,²³ A. Varganov,³⁵ E. Vataga,³⁸ F. Vázquezⁱ,¹⁸ G. Velev,¹⁷ G. Veramendi,²⁴
 V. Veszpremi,⁴⁹ R. Vidal,¹⁷ I. Vila,¹¹ R. Vilar,¹¹ T. Vine,³¹ I. Vollrath,³⁴ I. Volobouevⁿ,²⁹ G. Volpi,⁴⁷
 F. Würthwein,⁹ P. Wagner,⁵⁴ R.G. Wagner,² R.L. Wagner,¹⁷ J. Wagner,²⁶ W. Wagner,²⁶ R. Wallny,⁸
 S.M. Wang,¹ A. Warburton,³⁴ S. Waschke,²¹ D. Waters,³¹ M. Weinberger,⁵⁴ W.C. Wester III,¹⁷
 B. Whitehouse,⁵⁷ D. Whiteson,⁴⁶ A.B. Wicklund,² E. Wicklund,¹⁷ G. Williams,³⁴ H.H. Williams,⁴⁶
 P. Wilson,¹⁷ B.L. Winer,⁴⁰ P. Wittich^d,¹⁷ S. Wolbers,¹⁷ C. Wolfe,¹³ T. Wright,³⁵ X. Wu,²⁰
 S.M. Wynne,³⁰ A. Yagil,¹⁷ K. Yamamoto,⁴² J. Yamaoka,⁵³ T. Yamashita,⁴¹ C. Yang,⁶¹ U.K. Yang^j,¹³
 Y.C. Yang,²⁸ W.M. Yao,²⁹ G.P. Yeh,¹⁷ J. Yoh,¹⁷ K. Yorita,¹³ T. Yoshida,⁴² G.B. Yu,⁵⁰ I. Yu,²⁸
 S.S. Yu,¹⁷ J.C. Yun,¹⁷ L. Zanello,⁵² A. Zanetti,⁵⁵ I. Zaw,²² X. Zhang,²⁴ J. Zhou,⁵³ and S. Zucchelli⁵
 (CDF Collaboration*)

¹Institute of Physics, Academia Sinica, Taipei, Taiwan 11529, Republic of China

²Argonne National Laboratory, Argonne, Illinois 60439

³Institut de Fisica d'Altes Energies, Universitat Autònoma de Barcelona, E-08193, Bellaterra (Barcelona), Spain

⁴Baylor University, Waco, Texas 76798

⁵Istituto Nazionale di Fisica Nucleare, University of Bologna, I-40127 Bologna, Italy

⁶Brandeis University, Waltham, Massachusetts 02254

⁷University of California, Davis, Davis, California 95616

⁸University of California, Los Angeles, Los Angeles, California 90024

⁹University of California, San Diego, La Jolla, California 92093

¹⁰University of California, Santa Barbara, Santa Barbara, California 93106

¹¹Instituto de Fisica de Cantabria, CSIC-University of Cantabria, 39005 Santander, Spain

¹²Carnegie Mellon University, Pittsburgh, PA 15213
¹³Enrico Fermi Institute, University of Chicago, Chicago, Illinois 60637
¹⁴Comenius University, 842 48 Bratislava, Slovakia; Institute of Experimental Physics, 040 01 Kosice, Slovakia
¹⁵Joint Institute for Nuclear Research, RU-141980 Dubna, Russia
¹⁶Duke University, Durham, North Carolina 27708
¹⁷Fermi National Accelerator Laboratory, Batavia, Illinois 60510
¹⁸University of Florida, Gainesville, Florida 32611
¹⁹Laboratori Nazionali di Frascati, Istituto Nazionale di Fisica Nucleare, I-00044 Frascati, Italy
²⁰University of Geneva, CH-1211 Geneva 4, Switzerland
²¹Glasgow University, Glasgow G12 8QQ, United Kingdom
²²Harvard University, Cambridge, Massachusetts 02138
²³Division of High Energy Physics, Department of Physics, University of Helsinki and Helsinki Institute of Physics, FIN-00014, Helsinki, Finland
²⁴University of Illinois, Urbana, Illinois 61801
²⁵The Johns Hopkins University, Baltimore, Maryland 21218
²⁶Institut für Experimentelle Kernphysik, Universität Karlsruhe, 76128 Karlsruhe, Germany
²⁷High Energy Accelerator Research Organization (KEK), Tsukuba, Ibaraki 305, Japan
²⁸Center for High Energy Physics: Kyungpook National University, Taegu 702-701, Korea; Seoul National University, Seoul 151-742, Korea; and SungKyunKwan University, Suwon 440-746, Korea
²⁹Ernest Orlando Lawrence Berkeley National Laboratory, Berkeley, California 94720
³⁰University of Liverpool, Liverpool L69 7ZE, United Kingdom
³¹University College London, London WC1E 6BT, United Kingdom
³²Centro de Investigaciones Energeticas Medioambientales y Tecnologicas, E-28040 Madrid, Spain
³³Massachusetts Institute of Technology, Cambridge, Massachusetts 02139
³⁴Institute of Particle Physics: McGill University, Montréal, Canada H3A 2T8; and University of Toronto, Toronto, Canada M5S 1A7
³⁵University of Michigan, Ann Arbor, Michigan 48109
³⁶Michigan State University, East Lansing, Michigan 48824
³⁷Institution for Theoretical and Experimental Physics, ITEP, Moscow 117259, Russia
³⁸University of New Mexico, Albuquerque, New Mexico 87131
³⁹Northwestern University, Evanston, Illinois 60208
⁴⁰The Ohio State University, Columbus, Ohio 43210
⁴¹Okayama University, Okayama 700-8530, Japan
⁴²Osaka City University, Osaka 588, Japan
⁴³University of Oxford, Oxford OX1 3RH, United Kingdom
⁴⁴University of Padova, Istituto Nazionale di Fisica Nucleare, Sezione di Padova-Trento, I-35131 Padova, Italy
⁴⁵LPNHE, Université Pierre et Marie Curie/IN2P3-CNRS, UMR7585, Paris, F-75252 France
⁴⁶University of Pennsylvania, Philadelphia, Pennsylvania 19104
⁴⁷Istituto Nazionale di Fisica Nucleare Pisa, Universities of Pisa, Siena and Scuola Normale Superiore, I-56127 Pisa, Italy
⁴⁸University of Pittsburgh, Pittsburgh, Pennsylvania 15260
⁴⁹Purdue University, West Lafayette, Indiana 47907
⁵⁰University of Rochester, Rochester, New York 14627
⁵¹The Rockefeller University, New York, New York 10021
⁵²Istituto Nazionale di Fisica Nucleare, Sezione di Roma 1, University of Rome "La Sapienza," I-00185 Roma, Italy
⁵³Rutgers University, Piscataway, New Jersey 08855
⁵⁴Texas A&M University, College Station, Texas 77843
⁵⁵Istituto Nazionale di Fisica Nucleare, University of Trieste/ Udine, Italy
⁵⁶University of Tsukuba, Tsukuba, Ibaraki 305, Japan
⁵⁷Tufts University, Medford, Massachusetts 02155
⁵⁸Waseda University, Tokyo 169, Japan
⁵⁹Wayne State University, Detroit, Michigan 48201
⁶⁰University of Wisconsin, Madison, Wisconsin 53706
⁶¹Yale University, New Haven, Connecticut 06520

(Dated: February 8, 2020)

A search for a manifestly exotic $S = -2$ baryon state decaying to $\Xi^- \pi^-$, and its neutral partner decaying to $\Xi^- \pi^+$, has been performed using 220 pb $^{-1}$ of $p\bar{p}$ collisions at $\sqrt{s} = 1.96$ TeV collected by

the Collider Detector at Fermilab. The Ξ^- trajectories were measured in a silicon tracker before their decay, resulting in a sample with low background and excellent position resolution. No evidence was found for $S = -2$ pentaquark candidates in the invariant mass range of 1600 – 2100 MeV/ c^2 . Upper limits on the product of pentaquark production cross section times its branching fraction to $\Xi^- \pi^{+,-}$, relative to the cross section of the well established $\Xi(1530)$ resonance, are presented for neutral and doubly negative candidates with $p_T > 2$ GeV/ c and $|y| < 1$ as a function of pentaquark mass. At 1862 MeV/ c^2 , these upper limits for neutral and doubly negative final states were found to be 3.2% and 1.7% at the 90% confidence level, respectively.

PACS numbers: 13.85.Rm, 14.20.-c

Searches for hadrons characterized by exotic quantum numbers, i.e., quantum numbers that cannot be obtained from minimal quark-antiquark or three quark configurations of standard mesons and baryons, have taken place since the outset of the quark model. Until recently these searches yielded little evidence for such states. Most notably in the 1960's and 1970's there were searches for a Z^* -baryon with positive strangeness in bubble chamber experiments with incident beams of pions and kaons, which ended with negative results. These earlier searches are summarized in detailed reviews by Hey and Kelly [1] and more recently by Jennings and Maltman [2].

During 2003, however, the situation changed dramatically. A narrow resonance, decaying to nK^+ , was reported by the LEPS Collaboration in their study of exclusive photon-nucleon reactions [3]. A state decaying to nK^+ must have positive strangeness, an exotic quantum number for a baryon, and therefore cannot exist in a three-quark model. A pentaquark interpretation was employed, suggesting its quark contents to be $uudd\bar{s}$. The mass of the resonance was measured to be (1540 ± 10) MeV/ c^2 , in remarkable agreement with the theoretical prediction for the Θ^+ state made in the framework of the chiral soliton model by Diakonov, Petrov, and Polyakov [4]. Various experiments, using incident beams of real and quasi-real photons, kaons, and neutrons, claimed to confirm the initial reports of Θ^+ decaying to nK^+ and pK_S^0 [5, 6, 7, 8, 9, 10, 11, 12, 13].

Another manifestly exotic state, a doubly negative baryon decaying to $\Xi^- \pi^-$ [14], and its neutral partner decaying to $\Xi^- \pi^+$, were reported by

the NA49 Collaboration in $\sqrt{s} = 17.2$ GeV pp collisions at the CERN SPS [15]. These states have been tentatively labeled Φ^{--} and Φ^0 respectively, and the mass of the combined Φ^{--} and Φ^0 signals was measured to be (1862 ± 2) MeV/ c^2 . These resonances were interpreted as the $I_3 = -3/2$ and the $I_3 = +1/2$ partners of an isospin quadruplet of five-quark states with quark contents $dsds\bar{u}$ and $dsus\bar{d}$, respectively. No independent confirmation of these states exists.

All ostensible pentaquark signals are based on relatively small data samples. Typically 20 – 100 signal events are seen with estimated significances ranging from three to five standard deviations. With the exception of the ZEUS and HERMES Collaborations, which both have reported observations of Θ^+ in the pK_S^0 mode, many searches for strange pentaquark states produced in high-energy, high-statistics, fixed target or collider experiments have yielded negative results [16, 17, 18, 19, 20, 21, 22, 23, 24, 25, 26, 27, 28, 29, 30, 31, 32]. More recently, a high statistics analysis of the exclusive reaction $\gamma p \rightarrow \bar{K}^0 K^+ n$ performed by CLAS, which was one of the experiments initially reporting the observation of the Θ^+ , yielded no evidence for this state [33].

We report the results of searches for exotic baryons $\Phi^{0,--}$, decaying to $\Xi^- \pi^{+,-}$, in $p\bar{p}$ collisions at $\sqrt{s} = 1.96$ TeV. The data were recorded with the CDF II detector at the Fermilab Tevatron and correspond to 220 pb^{-1} of integrated luminosity.

The CDF II detector is described in detail elsewhere [34]. The aspects of the detector most relevant to this analysis are the tracking and the three-stage triggering systems. The tracking system lies within a superconducting solenoid, which provides a uniform axial magnetic field of 1.4 T. A system of double-sided micro-strip silicon sensors (SVX II) [35] is arranged in five concentric cylindrical shells with radii between 2.5 and 10.6 cm from the beamline [36], and approximately 90 cm in length. Each silicon layer contains axial strips to measure track positions in the plane transverse to the beam-line. Stereo measurements of $\pm 1.2^\circ$ and 90° with respect

*With visitors from ^aUniversity of Athens, ^bUniversity of Bristol, ^cUniversity Libre de Bruxelles, ^dCornell University, ^eUniversity of Cyprus, ^fUniversity of Dublin, ^gUniversity of Edinburgh, ^hUniversity of Heidelberg, ⁱUniversidad Iberoamericana, ^jUniversity of Manchester, ^kNagasaki Institute of Applied Science, ^lUniversity de Oviedo, ^mUniversity of London, Queen Mary and Westfield College, ⁿTexas Tech University, ^oIFIC(CSIC-Universitat de Valencia),

to the beam-line are also available. The remainder of the magnetic volume is occupied by a drift chamber, known as the central outer tracker (COT) [37]. The COT has a radial extent from 40 to 137 cm, and extends 3.1 m along the direction of the beam. The sense wires are arranged in 8 super layers of 12 wires each, which alternate between axial and $\pm 2^\circ$ stereo measurements to provide tracking in three dimensions.

The CDF II detector does not have a dedicated trigger selection for Φ pentaquark production. We therefore chose data sets obtained by two complementary types of triggers. The first dataset consists of the largest number of inelastic $p\bar{p}$ collisions recorded by the experiment, and is based on a displaced-track trigger, even though the Φ decay products usually produce tracks that have either too small or too large a displacement relative to the primary vertex to satisfy the trigger requirements. The second sample is obtained by a calorimeter-based jet trigger. This trigger has the merit of being largely independent of the pentaquark production and decay properties relevant to the displaced-track trigger. However, due to its low jet-energy threshold, only a relatively small fraction of such triggers could be recorded, thereby limiting its statistical sensitivity for this search.

The displaced-track trigger was designed primarily for recording hadronic B-decays. This trigger requires the presence in the event of a pair of oppositely charged tracks identified in the transverse view by a fast hardware track fitter called the silicon vertex trigger (SVT) [38]. Each track is required to have transverse momentum $p_T > 2.0 \text{ GeV}/c$, and an impact parameter (d_0) which falls within the range $120 \mu\text{m} < |d_0| < 1 \text{ mm}$ [39]. In addition, the intersection point of the triggered track pair is required to have a $200 \mu\text{m}$ transverse displacement with respect to the beam-line, the scalar sum of the two transverse momenta must exceed $5.5 \text{ GeV}/c$, and the azimuthal angular difference between the tracks is required to be within the range $2^\circ < \Delta\phi < 90^\circ$.

The calorimeter based trigger requires the presence of a jet with transverse energy $E_T > 20 \text{ GeV}$ (the Jet20 trigger). The CDF II calorimeter system covers a pseudorapidity region of $|\eta| < 3.5$ [36] and consists of electromagnetic and hadronic sections [40]. The physical towers are grouped into trigger towers that span 15° in ϕ and approximately 0.2 in η for central towers ($|\eta| < 1.0$). The level-1 trigger requires a single tower with an $E_T > 5 \text{ GeV}$. At level 2, a calorimeter cluster is required to have an E_T above 15 GeV . The level-3 trigger uses a jet cone algorithm to reconstruct jets with a cone size $R = \sqrt{\Delta\eta^2 + \Delta\phi^2} < 0.7$ around a seed tower

[41]. Due to trigger rate limitations, the jet trigger is prescaled such that this dataset contains an effective integrated luminosity of only about 0.52 pb^{-1} .

Pentaquark candidates were reconstructed through the decay chain: $\Phi^{0,--} \rightarrow \Xi^-\pi^{+,-}$, $\Xi^- \rightarrow \Lambda\pi^-$ and $\Lambda \rightarrow p\pi^-$. Our reconstruction and selection strategy was guided by using the $\Xi(1530) \rightarrow \Xi^-\pi^+$ signal in our data as a model for Φ production. The Λ candidates were reconstructed from oppositely charged pairs of tracks that had more than 20 axial and 16 stereo COT hits and an impact parameter greater than $500 \mu\text{m}$. The track with the highest transverse momentum in the pair was assigned the proton mass. This assignment is always correct for true Λ candidates whose decay products have sufficient p_T to be measured by the tracking system. A vertex constrained fit of track pairs was performed for the Λ candidates. The invariant mass was required to be within $\pm 5 \text{ MeV}/c^2$ of the world average Λ mass, and the vertex displacement in the transverse plane was required to be greater than 1 cm from the beam-line.

The Ξ^- hyperons were reconstructed in the decay chain $\Xi^- \rightarrow \Lambda\pi^-$ by combining Λ candidates with each remaining negative track, assumed to be pion, in the event. The track parameters of each three-track combination were refit with a Ξ^- decay hypothesis, including a mass constraint to the Λ mass ($1115.683 \text{ MeV}/c^2$) [42] on the tracks originating from the Λ candidate. Candidates that were consistent with this hypothesis, and had a total invariant mass within $60 \text{ MeV}/c^2$ of the Ξ^- mass ($1321.31 \text{ MeV}/c^2$) [42], were refit with a Ξ^- mass constraint. The Ξ^- decay vertex was required to be closer to the primary vertex than the Λ decay vertex, and we required at least 1 cm radial separation between the two decay vertices.

The lifetime of the Ξ^- , $c\tau = (4.91 \pm 0.04) \text{ cm}$ [42], and the p_T requirements resulting from our acceptance, produce a Ξ^- decay vertex that lies outside the inner layers of the SVX II for a majority of the events. This makes it possible to reconstruct the Ξ^- track from the hits left in the layers of the SVX II. The momentum and decay vertex of the Ξ^- candidate as reconstructed in the COT were used to define its track helix. Hits in the SVX II detector made by real Ξ^- hyperons are expected to fall near the extrapolation of this helix in the silicon detector. A dedicated tracking algorithm was used to attach hits in the SVX II to the Ξ^- helix, which required a minimum of two axial silicon hits. The hyperon tracks found in the SVX II were used, with Ξ^- mass assignment, in the subsequent analysis in the same way as standard tracks produced by stable

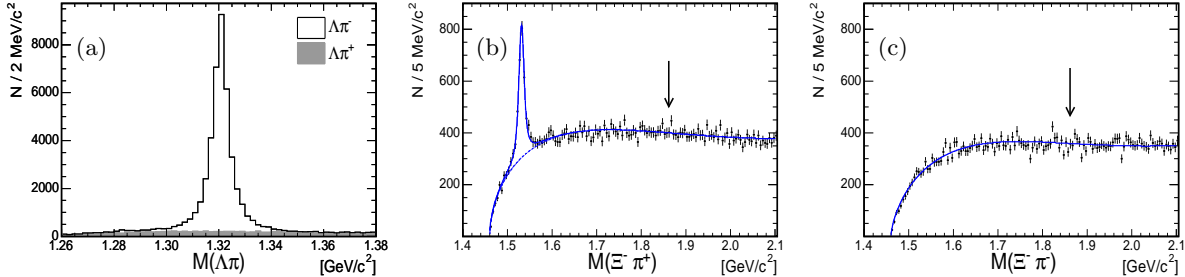


FIG. 1: Invariant mass spectra from the SVT sample for: (a) $\Lambda\pi^\mp$ candidates that have an associated Ξ^- track in the SVX II, where the open histogram shows right-sign $\Lambda\pi^-$ combinations, and the filled histogram shows wrong-sign $\Lambda\pi^+$ combinations; (b) $\Xi^-\pi^+$ combinations, which display a clear $\Xi(1530)$ peak; and (c) $\Xi^-\pi^-$ combinations. Arrows mark the mass at $1862 \text{ MeV}/c^2$, where the NA49 Collaboration reported observing the Φ . The smooth curves represent fits to the spectra and are described in the text.

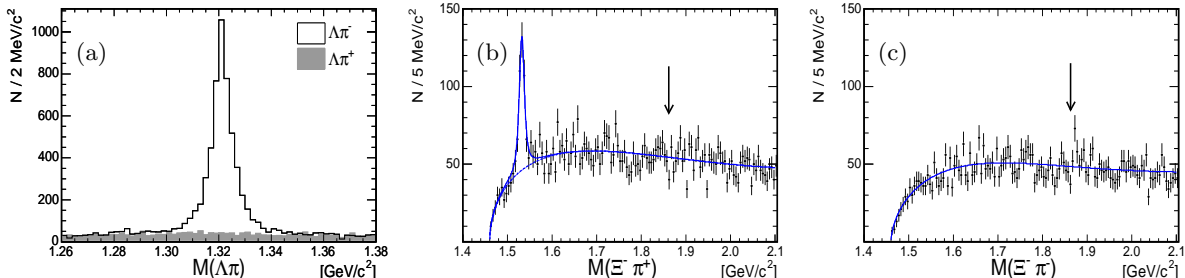


FIG. 2: Invariant mass spectra from the Jet20 sample for: (a) $\Lambda\pi^\mp$ candidates that have an associated Ξ^- track, where the open (filled) histogram is right-sign $\Lambda\pi^-$ (wrong-sign $\Lambda\pi^+$) combinations; (b) $\Xi^-\pi^+$ combinations; and (c) $\Xi^-\pi^-$ combinations. Arrows mark $1862 \text{ MeV}/c^2$, and the smooth curves represent fits described in the text.

particles.

The $\Lambda\pi^-$ invariant mass spectrum of Ξ^- candidates found in the SVT dataset is shown in Fig. 1(a). A Ξ^- signal containing about 36,000 candidates is evident. The invariant mass spectrum of wrong-charge combinations, $\Lambda\pi^+$, shown by the filled histogram, provides a good description of the right-sign combinatorial background. No artificial signal was created by the selection criteria or the hyperon tracking procedure.

To search for new states, each Ξ^- candidate was combined with all remaining tracks. These tracks were assigned the pion mass and were required to have $p_T > 0.4 \text{ GeV}/c$, at least 20 axial and at least 20 stereo COT hits, and 3 or more axial SVX II hits. In addition, Ξ^- tracks and pion tracks were required to have impact parameters that were smaller than 0.015 cm and 0.1 cm respectively. The remaining $\Xi^-\pi^\pm$ pairs were subjected to a common vertex fit with the total momentum of the pair constrained to point back to the primary vertex in the transverse plane. A vertex fit quality requirement was imposed, so that only well measured candidates

were retained for further analysis.

No additional kinematic cuts were applied to $\Xi^-\pi^\pm$ pairs. As described earlier, such states are unlikely to produce track pairs satisfying the SVT trigger criteria. Therefore, $\Xi^-\pi^\pm$ candidates were not required to satisfy the SVT trigger. Since the SVT trigger selects events containing particles produced in the decays of long-lived Λ baryons, our source of pentaquark candidates would be predominantly the fragmentation of the available light quarks in the event, as is the case for $\Xi(1530)$ baryons.

The invariant mass spectra of $\Xi^-\pi^+$ and $\Xi^-\pi^-$ combinations are shown in Figs. 1(b) and (c) respectively. A prominent peak corresponding to the decay $\Xi(1530) \rightarrow \Xi^-\pi^+$ is clearly visible in the $\Xi^-\pi^+$ mass distribution. No other narrow structures can be seen in either distribution. The smooth curves superimposed on the $\Xi^-\pi^\pm$ spectra show the results of unbinned maximum-likelihood fits to the data. The fit function included a Breit-Wigner resonance shape convoluted with a Gaussian resolution function describing the $\Xi(1530)$, plus a third de-

gree polynomial multiplied by an exponential as a model for the background. The width of the Gaussian was allowed to float, and the intrinsic width of the $\Xi(1530)$ was Gaussian-constrained in the fit to the world average value of $(9.1 \pm 0.5) \text{ MeV}/c^2$ [42]. The fit yielded $1923 \pm 80(\text{stat})$ candidates above the background at a mass of $(1531.7 \pm 0.3(\text{stat})) \text{ MeV}/c^2$, in excellent agreement with world average mass of the $\Xi(1530)$. The fitted mass resolution of $(3.5 \pm 0.6(\text{stat})) \text{ MeV}/c^2$ is in agreement with the expected mass resolution based on the full detector simulation. No excess of events appears at a mass of $1862 \text{ MeV}/c^2$, the mass claimed by NA49 for the Φ states. Since the production mechanism of pentaquark states is unknown, it is possible that the SVT trigger bias may preferentially reject events with pentaquarks. To address this issue, an identical analysis has been performed using the data obtained with the Jet20 trigger.

The invariant mass spectra of $\Lambda\pi^-$ and $\Lambda\pi^+$ combinations reconstructed in the Jet20 data and having an associated SVX II hyperon track are shown in Fig. 2(a). The jet-trigger data sample is significantly smaller than the data sample obtained with the trigger on displaced tracks. However, this sample of $4870 \pm 128(\text{stat}) \Xi^-$ candidates is still a factor of 2.5 times larger than the sample used by the NA49 experiment in their analysis. The $\Xi^-\pi^+$ and $\Xi^-\pi^-$ invariant mass spectra are shown in Figs. 2(b) and (c). Again, the baryon $\Xi(1530)$ is seen, and no narrow structures are visible at the mass of $1862 \text{ MeV}/c^2$. The $\Xi^-\pi^+$ invariant mass spectrum was fit in a similar fashion as previously described with the exception that the Gaussian resolution of the $\Xi(1530)$ peak was constrained to $(3.5 \pm 0.6) \text{ MeV}/c^2$. The fit yielded a signal of $313 \pm 28(\text{stat}) \Xi(1530)$ candidates.

There is no indication of $S = -2$ pentaquark production in these data. We determined an upper limit on the Φ pentaquark cross section times the branching fraction $\mathcal{B}(\Phi \rightarrow \Xi^-\pi^\pm)$ relative to the $\Xi(1530)$ cross section in $p\bar{p}$ collisions. Knowledge of this ratio can be an important input for pentaquark production models. Since the two states share the same final state, many sources of systematic uncertainty cancel out in this ratio. We measured this ratio for the Φ mass of $(1862 \pm 2) \text{ MeV}/c^2$, the value reported by the NA49 Collaboration, and performed a scan of this ratio in the mass range $[1600\text{--}2100] \text{ MeV}/c^2$.

Relative acceptances and reconstruction efficiencies for $\Xi^-\pi^\pm$ final states of different invariant mass have been studied with $p\bar{p} \rightarrow b\bar{b}\Xi(1530)X$ events produced with the PYTHIA event generator [43] and subjected to the full GEANT simulation of the CDF

II detector, trigger, and reconstruction. The pentaquark states were represented in the PYTHIA decay table as $\Xi(1530)$ with various masses. The pentaquarks were not required to originate from hadrons containing a Λ or Ξ quark. The simulation of the associated production with $b\bar{b}$ pairs is a purely practical approach to satisfy SVT trigger conditions. Four samples were generated for masses of $1530, 1696, 1862$, and $2027 \text{ MeV}/c^2$ in order to obtain the mass dependence of the detector resolution and detector efficiency for the whole mass range of interest. The generated p_T spectrum of the $\Xi(1530)$ was re-weighted to reproduce the p_T distribution of the $\Xi(1530)$ measured in the SVT trigger data [44]. The latter is shown in Fig. 3. The smooth curve shows a fit with an exponential convoluted with a Gaussian. The same weight function was applied to the p_T spectra of the generated pentaquarks in all four samples. Lacking any established model for pentaquark production, we assumed that the p_T spectrum of the Φ pentaquark is the same as that of the $\Xi(1530)$, other than the kinematic effects of heavier masses in the PYTHIA generation.

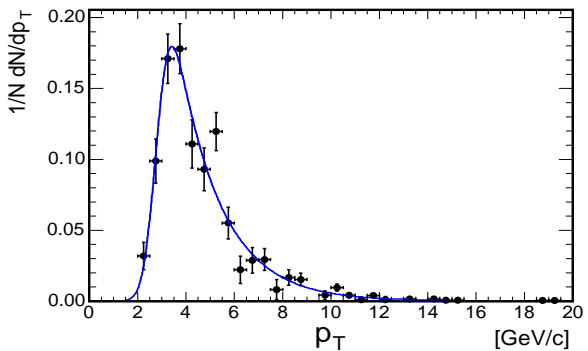


FIG. 3: Reconstructed transverse momentum spectrum of the $\Xi(1530)$. The fit function is described in the text.

The sensitivity of the experiment to $\Xi^-\pi^\pm$ final states is limited by our tracking acceptance to particles that have transverse momentum greater than $2 \text{ GeV}/c$ and $|y| \leq 1$. Compared to the $\Xi(1530)$, a pentaquark with a mass of $1862 \text{ MeV}/c^2$ would have a factor of 1.5 higher detection efficiency at $p_T = 2 \text{ GeV}/c$; this ratio of efficiencies decreases with increasing p_T . We estimate that the ratio of detector efficiencies averaged over the range of p_T within our acceptance is $1.29 \pm 0.05(\text{stat})$, where the uncertainty is due to the size of the simulated event sample. There is an additional 10% systematic uncertainty due to the parameterization of the $\Xi(1530)$ transverse momentum. This value is obtained by varying the parameters of the fit to the observed

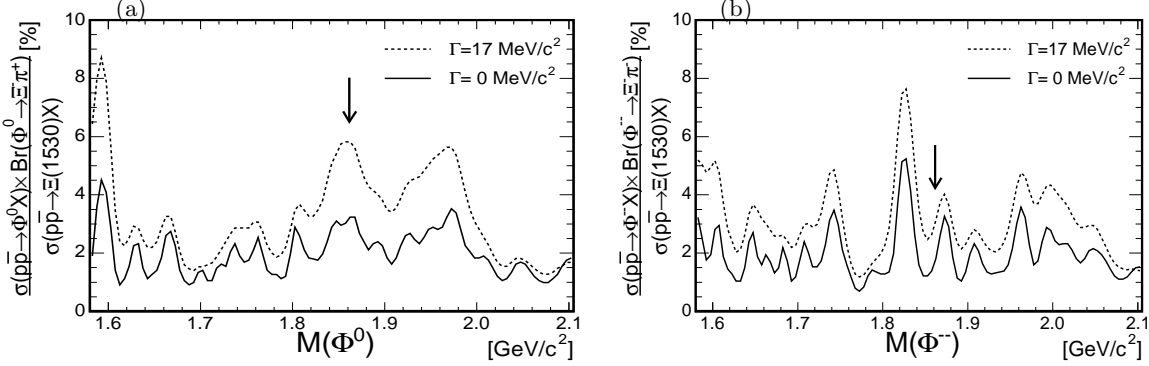


FIG. 4: Upper limits from SVT data (90% confidence level) for the production cross section of Φ pentaquarks times the $\Phi \rightarrow \Xi\pi$ branching ratios relative to the $\Xi(1530)$ cross section as a function of: (a) Φ^0 mass, and (b) Φ^{--} mass. The solid line shows the results obtained assuming zero natural width of the pentaquark, and the dashed line shows the results obtained assuming $\Gamma = 17$ MeV/c 2 . The arrows mark the position of the NA49 peak.

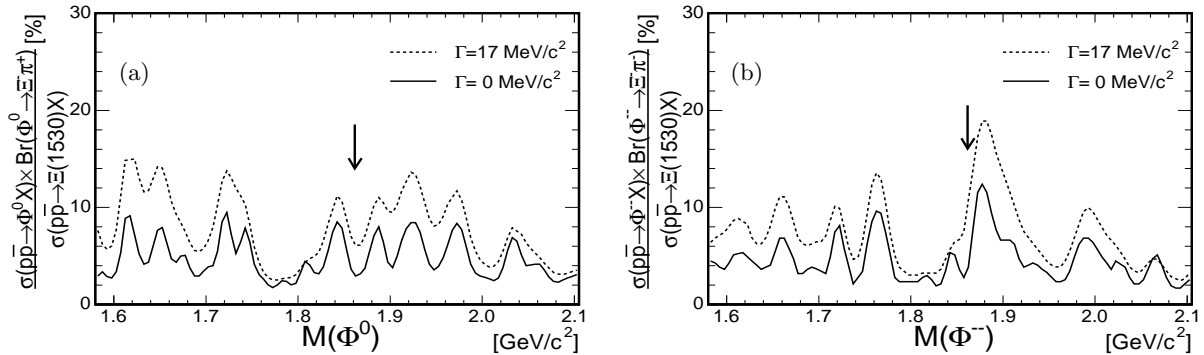


FIG. 5: Upper limits from Jet20 data (90% confidence level) for the production cross section of Φ pentaquarks times the $\Phi \rightarrow \Xi\pi$ branching ratios relative to the $\Xi(1530)$ cross section as a function of: (a) Φ^0 mass, and (b) Φ^{--} mass. The solid (dashed) line shows the results obtained assuming $\Gamma = 0$ (17) MeV/c 2 . The arrows mark the position of the NA49 peak.

$\Xi(1530)$ p_T spectrum within statistical errors, and re-weighting the input spectrum of the simulation accordingly.

The limits on $\sigma(p\bar{p} \rightarrow \Phi^{0,--}X) \cdot \mathcal{B}(\Phi^{0,--} \rightarrow \Xi^-\pi^{+,-})/\sigma(p\bar{p} \rightarrow \Xi(1530)X)$ were obtained by introducing an additional signal term for the hypothetical pentaquark signal, represented by a Breit-Wigner resonance shape convoluted with a Gaussian resolution, into the previously described fit function. The expected detector resolution at $m(\Xi^-\pi^\pm) = 1862$ MeV/c 2 is $(6.6 \pm 0.7\text{stat}) \pm 0.5\text{syst})$ MeV/c 2 , which was obtained through detector simulation. The presence of a Φ signal was evaluated for two hypotheses for its natural width: a natural width of zero, and a natural width equal to 17 MeV/c 2 , the latter value being the measured full width at half maximum of the peak reported

by the NA49 Collaboration [15]. The values of the relative efficiency and the mass resolution at $m(\Phi) = 1862$ MeV/c 2 were allowed to vary by their uncertainties by adding a Gaussian constraint to the likelihood function. The widths of the Gaussians were set to the sum in quadrature of the statistical and systematic uncertainties. We determined the limit on the production of the Φ observed by the NA49 Collaboration by imposing their measured mass with a Gaussian constraint of 2 MeV/c 2 in the likelihood. The limits are established using a Bayesian approach, with a uniform prior for the relative production cross section, and taking into account $\mathcal{B}(\Xi(1530) \rightarrow \Xi^-\pi^+) = 0.67$ [42]. The limits at the 90% confidence level are summarized in Table I.

Available predictions for $S = -2$ pentaquark

	SVT trigger	Jet20 trigger
$N(\Xi^-)$	35722 ± 326	4870 ± 122
$N(\Xi(1530))$	1923 ± 80	313 ± 28
$\frac{\sigma(p\bar{p} \rightarrow \Phi^0 X) \cdot \mathcal{B}(\Phi^0 \rightarrow \Xi^- \pi^+)}{\sigma(p\bar{p} \rightarrow \Xi(1530) X)} [\%]$	< 3.2 (5.8)	< 3.0 (9.2)
$\frac{\sigma(p\bar{p} \rightarrow \Phi^{--} X) \cdot \mathcal{B}(\Phi^{--} \rightarrow \Xi^- \pi^-)}{\sigma(p\bar{p} \rightarrow \Xi(1530) X)} [\%]$	< 1.7 (3.1)	< 3.2 (10.1)

TABLE I: Event yields of Ξ^- , $\Xi(1530)$, and upper limits on $\sigma(p\bar{p} \rightarrow \Phi^{0,--} X) \cdot \mathcal{B}(\Phi^{0,--} \rightarrow \Xi^- \pi^{+,-})/\sigma(p\bar{p} \rightarrow \Xi(1530) X)$ for $m(\Phi) = (1862 \pm 2) \text{ MeV}/c^2$, at 90% confidence levels obtained by assuming zero natural width of the pentaquarks. Numbers in parentheses were calculated with the assumption of a $17 \text{ MeV}/c^2$ natural width.

masses vary over a range from 1750 to $2027 \text{ MeV}/c^2$ [4, 45, 46, 47]. Since we failed to see evidence for a signal at the mass stated by the NA49 Collaboration, we have also derived a limit on the relative pentaquark production rate as a function of mass in the range $[1600\text{--}2100] \text{ MeV}/c^2$ in order to provide a generic bound on Φ pentaquark production models. The procedure to determine the upper limit on the relative cross section for a pentaquark mass within the range $[1600\text{--}2100] \text{ MeV}/c^2$ was similar to the one used for testing the NA49 Collaboration's observation. We performed a fit for the relative cross section over this mass range in $2 \text{ MeV}/c^2$ steps in pentaquark mass. The relative detection efficiency and mass resolution entered as a function of mass into the fit function. The results of the relative cross section scans for neutral and doubly negative pentaquarks are shown in Figs. 4 and 5. Neither the SVT trigger data nor the Jet20 trigger data show evidence for pentaquarks over this broad mass range.

In conclusion, we have performed a search for exotic $S = -2$ baryon states decaying to $\Xi^- \pi^-$ and $\Xi^- \pi^+$ over the mass range of $[1600\text{--}2100] \text{ MeV}/c^2$. No evidence for a signal has been found, and we have set upper limits on the relative cross section times branching fraction of exotic cascade baryons with respect to the well established resonance $\Xi(1530)$ for $p_T > 2 \text{ GeV}/c$ and $|y| < 1$. We summarize our results by quoting the higher statistics analysis with the displaced-track trigger, in which $\sigma(p\bar{p} \rightarrow$

$\Phi X) \cdot \mathcal{B}(\Phi^{0,--} \rightarrow \Xi^- \pi^{+,-})/\sigma(p\bar{p} \rightarrow \Xi(1530) X)$ for neutral and doubly negative states were respectively found to be less than 3.2% and 1.7% at the 90% confidence level, for the mass reported by the NA49 Collaboration [15]. Consequently, we find that these data are unable to confirm the existence of exotic $S = -2$ baryons.

We thank the Fermilab staff and the technical staffs of the participating institutions for their vital contributions. This work was supported by the U.S. Department of Energy and National Science Foundation; the Italian Istituto Nazionale di Fisica Nucleare; the Ministry of Education, Culture, Sports, Science and Technology of Japan; the Natural Sciences and Engineering Research Council of Canada; the National Science Council of the Republic of China; the Swiss National Science Foundation; the A.P. Sloan Foundation; the Bundesministerium für Bildung und Forschung, Germany; the Korean Science and Engineering Foundation and the Korean Research Foundation; the Particle Physics and Astronomy Research Council and the Royal Society, UK; the Institut National de Physique Nucléaire et Physique des Particules/CNRS; the Russian Foundation for Basic Research; the Comisión Interministerial de Ciencia y Tecnología, Spain; the European Community's Human Potential Programme under contract HPRN-CT-2002-00292; and the Academy of Finland.

[1] A. J. G. Hey and R. L. Kelly, Phys. Rep. **96**, 71 (1983).
 [2] B. K. Jennings and K. Maltman, Phys. Rev. D **69**, 094020 (2004).
 [3] T. Nakano *et al.* (LEPS Collaboration), Phys. Rev. Lett. **91**, 012002 (2003).
 [4] D. Diakonov, V. Petrov and M. V. Polyakov, Z. Phys. A **359**, 305 (1997).
 [5] V. V. Barmin *et al.* (DIANA Collaboration), Phys. Atom. Nuclei **66**, 1715 (2003) [Yad. Fiz. **66**, 1763 (2003)].
 [6] S. Stepanyan *et al.* (CLAS Collaboration), Phys. Rev. Lett. **91**, 252001 (2003).
 [7] V. Kubarovsky *et al.* (CLAS Collaboration), Phys. Rev. Lett. **92**, 032001 (2004) [Erratum-*ibid.* **92**, 049902 (2004)].
 [8] M. Abdel-Bary *et al.* (COSY-TOF Collaboration), Phys. Lett. B **595**, 127 (2004).
 [9] A. Aleev *et al.* (SVD Collaboration), Phys. Atom. Nuclei **68**, 974 (2005) [Yad. Fiz. **68** 1012 (2005)].
 [10] J. Barth *et al.* (SAPHIR Collaboration), Phys. Lett.

B **572**, 127 (2003).

[11] A. E. Asratyan, A. G. Dolgolenko, and M. A. Kubantsev, Phys. Atom. Nuclei **67**, 682 (2004) [Yad. Fiz. **67**, 704 (2004)].

[12] A. Airapetian *et al.* (HERMES Collaboration), Phys. Lett. B **585**, 213 (2004).

[13] S. Chekanov *et al.* (ZEUS Collaboration), Phys. Lett. B **591**, 7 (2004).

[14] Unless otherwise noted, the charge conjugate state is implied.

[15] C. Alt *et al.* (NA49 Collaboration), Phys. Rev. Lett. **92**, 042003 (2004).

[16] B. Aubert *et al.* (BABAR Collaboration), in *Proceedings 32nd International Conference on High-Energy Physics (ICHEP 04)*, Beijing, China, 2004, edited by H. Chen *et al.*, World Scientific, 2005, hep-ex/0408037.

[17] M. J. Longo *et al.* (HyperCP Collaboration), Phys. Rev. D **70**, 111101 (2004).

[18] J. Z. Bai *et al.* (BES Collaboration), Phys. Rev. D **70**, 012004 (2004).

[19] I. Abt *et al.* (HERA-B Collaboration), Phys. Rev. Lett. **93**, 212003 (2004).

[20] S. Schael *et al.* (ALEPH Collaboration), Phys. Lett. B **599**, 1 (2004).

[21] B. Aubert *et al.* (BABAR Collaboration), in *Proceedings of 32nd International Conference on High-Energy Physics (ICHEP 04)*, Beijing, China, 2004 Edited by H. Chen *et al.*, World Scientific, 2005, hep-ex/0408064.

[22] K. Abe *et al.* (Belle Collaboration), in *Proceedings of International Workshop on PENTAQUARK04, Spring-8*, Hyogo, Japan, 2004, Nishiharima 2004, hep-ex/0411005

[23] K. Abe *et al.* (Belle Collaboration), Phys. Lett. B **632**, 173 (2006).

[24] K. Stenson *et al.* (FOCUS Collaboration), Int. J. Mod. Phys. A **20**, 3745 (2005).

[25] A. Airapetian *et al.* (HERMES Collaboration), Phys. Rev. D **71**, 032004 (2005).

[26] M. I. Adamovich *et al.* (WA89 Collaboration), Phys. Rev. C **70**, 022201 (2004).

[27] S. Chekanov *et al.* (ZEUS Collaboration), Phys. Lett. B **610**, 212 (2005).

[28] E. S. Ageev *et al.* (COMPASS Collaboration), Eur. Phys. J. C **41**, 469 (2005).

[29] E. P. Hartouni *et al.*, UMHEP-315, *Contribution to BNL Workshop on Glueballs, Hybrids and Exotic Hadrons*, Upton, N.Y., 1988.

[30] S. R. Armstrong (LEP Experiments), Nucl. Phys. Proc. Suppl. **142**, 364 (2005).

[31] D. C. Christian *et al.* (E690 Collaboration), Phys. Rev. Lett. **95**, 152001 (2005).

[32] B. Aubert *et al.* (BABAR Collaboration), Phys. Rev. Lett. **95**, 042002 (2005).

[33] M. Battaglieri *et al.* (CLAS Collaboration), Phys. Rev. Lett. **96**, 042001 (2006).

[34] D. Acosta *et al.* (CDF Collaboration), Phys. Rev. D **71**, 032001 (2005); F. Abe *et al.*, Nucl. Instrum. Methods A **271**, 387 (1988).

[35] A. Sill *et al.*, Nucl. Instr. Meth. A **447**, 1 (2000).

[36] CDF uses a cylindrical coordinate system about the proton beam axis in which θ is the polar angle, ϕ is the azimuthal angle, and the pseudorapidity is defined as $\eta = -\ln[\tan(\theta/2)]$. The true rapidity is $y = \frac{1}{2} \ln\left(\frac{E+p_z}{E-p_z}\right)$ where E is the energy of the particle and p_z is the projection of its momentum to z -axis.

[37] T. Affolder *et al.*, Nucl. Instr. Meth. A **526**, 249 (2004).

[38] E. J. Thomson *et al.*, IEEE Trans. Nucl. Sci. **49**, 1063 (2002); B. Ashmanskas *et al.*, Nucl. Instr. Meth. A **518**, 532 (2004).

[39] The impact parameter is the distance of closest approach between a track and the primary vertex in the transverse plane.

[40] L. Balka *et al.*, Nucl. Instr. Meth. A **267**, 272 (1988); S. Bertolucci *et al.*, Nucl. Instr. Meth. A **267**, 301 (1988).

[41] G. Arison *et al.* (UA1 Collaboration), Phys. Lett. B **123**, 115 (1983); F. Abe *et al.* (CDF Collaboration), Phys. Rev. D **45**, 1448 (1992).

[42] S. Eidelman *et al.* (Particle Data Group), Phys. Lett. B **592**, 1 (2004).

[43] T. Sjöstrand *et al.*, Comput. Phys. Commun. **135**, 238 (2001).

[44] The spectrum observed in the data is described by the exponential $dN/dp_T \propto \exp(-\alpha p_T)$ with $\alpha = 0.70 \text{ (GeV/c)}^{-1}$.

[45] R. L. Jaffe and F. Wilczek, Phys. Rev. Lett. **91**, 232003 (2003).

[46] J. R. Ellis, M. Karliner, and M. Praszalowicz, J. High Energy Phys. **0405**, 002 (2004).

[47] M. Karliner and H. J. Lipkin, Phys. Lett. B **594**, 273 (2004).